Hydrol. Earth Syst. Sci. Discuss., 9, 1163–1205, 2012
www.hydrol-earth-syst-sci-discuss.net/9/1163/2012/
doi:10.5194/hessd-9-1163-2012

Hydrology and Earth System Sciences Discussions

Coupling a groundwater model with a land surface model to improve water and energy cycle simulation

W. Tian[1], X. Li[1], X.-S. Wang[2], and B. X. Hu[2,3]

[1]Cold and Arid Regions Environmental and Engineering Research Institute, Chinese Academy of Sciences, Lanzhou, China
[2]School of Water Resources and Environment, China University of Geosciences (Beijing), Beijing, China
[3]Department of Geological Sciences, Florida State University, Tallahassee, FL 32306, USA

Received: 6 January 2012 – Accepted: 9 January 2012 – Published: 23 January 2012

Correspondence to: X. Li (lixin@lzb.ac.cn)

Published by Copernicus Publications on behalf of the European Geosciences Union.

Abstract

The water and energy cycles interact, making them generally closely related. Land surface models (LSMs) can describe the water and energy cycles of the land surface, but their description of the subsurface water processes is oversimplified, and lateral groundwater flow is ignored. Groundwater models (GWMs) well describe the dynamic movement of subsurface water flow, but they cannot depict the physical mechanism of the evapotranspiration (ET) process in detail. In this study, a coupled model of groundwater with simple biosphere (GWSiB) is developed based on the full coupling of a typical land surface model (SiB2) and a three-dimensional variably saturated groundwater model (AquiferFlow). In this model, the infiltration, ET and energy transfer are simulated by SiB2 via the soil moisture results given by the groundwater flow model. The infiltration and ET results are applied iteratively to drive the groundwater flow model. The developed model is then applied to study water cycle processes in the middle reaches of the Heihe River Basin in the northwest of China. The model is validated through data collected at three stations in the study area. The stations are located in a shallow groundwater depth zone, a deeper groundwater depth zone and an agricultural irrigation area. The study results show that the coupled model can well depict the land surface and groundwater interaction and can more comprehensively and accurately simulate the water and energy cycles compared with uncoupled models.

1 Introduction

Water movement and energy transfer in the soil-atmosphere-vegetation continuum are the main processes on the land surface, and the two processes strongly interact. Land surface models (LSMs) are often used to depict these physical processes. However, almost all LSMs are one-dimensional vertical models because the initial aim of these models was to provide a land surface condition for atmospheric models, such

HESSD
9, 1163–1205, 2012

as general circulation models (GCMs) or regional climate models. Therefore, these models generally cannot simulate subsurface lateral water movement. However, many studies have indicated that lateral water movement can significantly affect land surface water and energy processes (Holt et al., 2006; Maxwell et al., 2007, 2011; Kollet and Maxwell, 2008; Soylu et al., 2011).

Many groundwater models (GWMs), such as the MODFLOW-HYDRUS (Twarakavi et al., 2008) and ParFlow (Kollet and Maxwell, 2006), are based on hydrodynamic mechanisms. These models describe the physical mechanism of the three-dimensional subsurface water movement in both saturation and unsaturation zones and include water balance processes, but they usually do not explicitly describe the physical mechanism of evapotranspiration (ET) processes. ET is an integration process that includes water, energy and biological processes. The latter two processes are usually not included in GWMs. In MODFLOW (McDonald and Harbaugh, 1988), for example, ET is calculated with a linear empirical function of the groundwater table (GWT). Although this approach makes the groundwater modeling system self-closing, it oversimplifies the ET simulation, leading to simulation error.

Based on this analysis of the two kinds of models, coupling LSM and GWM could be a way to eliminate their disadvantages and make the simulation of water movement in Earth's surface more accurate. In recent years, many studies have been conducted on the coupling of GWMs with the LSMs. Gutowski et al. (2002) developed a Coupled Land-Atmosphere Simulation Program (CLASP) to study the coupled aquifer, land surface and atmospheric hydrological cycle. This model considers the groundwater as a reservoir. York et al. (2002) improved this model by integrating the soil vegetation zone routines into the USGS groundwater flow model, MODFLOW, thereby generating the CLASP II. Liang et al. (2003) developed a one-dimensional dynamic groundwater parameterization and implemented it into a three-layer variable infiltration capacity (VIC-3L) model to simulate surface and groundwater interaction dynamics for LSMs. Gedney and Cox (2003) coupled the Hadley Centre Atmospheric Climate Model (HadAM3) with the Met Office Surface Exchange Scheme (MOSES), in which the local

HESSD
9, 1163–1205, 2012

water table depth was taken into account to estimate the saturated fraction of soil layers and improve the runoff and global wetland area simulation. Yeh and Eltahir (2005) incorporated a lumped unconfined aquifer model into the land surface scheme (Land Surface Transfer Scheme, LSX) to address the deficiency of the simplified representation of subsurface hydrological processes in current land surface parameterization schemes. In the model, groundwater was thought of as a nonlinear reservoir, receiving the recharge from the overlying soils and discharging the runoff into streams. Niu et al. (2007) developed a simple groundwater model (SIMGM) by representing groundwater recharge and discharge processes, which are added as a single integration element below the soil of the land surface model (CLM3). Fan et al. (2007) coupled a simple two-dimensional groundwater flow model with the VIC to estimate the equilibrium water table, which is the result of long-term climatic and geologic forcing. Maxwell and Miller (2005) coupled the Common Land Model with a variably saturated GWM (ParFlow) to create a single-column model to improve groundwater representation in land surface schemes. Kollet and Maxwell (2008) then improved this model and developed an integrated, distributed watershed model based on the coupling of ParFlow and the Common Land Model (PF.CLM). Maxwell et al. (2011) coupled ParFlow with the Noah LSM, which is a land surface module of Weather Research and Forecasting (WRF), to study the impact of groundwater on weather. All these studies show that groundwater flow and land surface processes are closely related and that coupled models can simulate complex processes more realistically than uncoupled models.

The GWMs used in the above model couplings can be classified into two categories: empirical, lumped GWMs (Liang et al., 2003; Gedney and Cox, 2003; Yeh and Eltahir, 2005; Niu et al., 2007) and physically based distributed GWMs (York et al., 2002; Maxwell et al., 2011; Kollet and Maxwell, 2008; Gutowski et al., 2002; Fan et al., 2007). It is obvious that the lumped GWMs can only provide a groundwater impact factor for the LSMs and cannot truly describe groundwater flow. Distributed dynamic GWMs, however, can explicitly depict groundwater flow and can be integrated with the water movement of LSMs. In particular, the PF.CLM model integrates the groundwater

HESSD
9, 1163–1205, 2012

flow in saturated and unsaturated zones with surface water movement from physical mechanisms.

In this paper, a coupled model of groundwater with simple biosphere (GWSiB) is developed based on coupling a three-dimensional variably saturated dynamic GWM (AquiferFlow) (Wang, 2007; Wang et al., 2010) with a typical land surface model, the Simple Biosphere Model version 2 (SiB2) (Sellers et al., 1996b). In our model-coupling system, the land surface parameterization scheme and GWM used are different from other studies. Furthermore, a more flexible temporal coupling method is added that increases the applicability of the model. The paper is arranged as follows. In Sect. 2, the models used for coupling are briefly introduced, and the coupled method of GWSiB is described in detail. In Sect. 3, a case study is conducted on the water and energy cycle processes in the middle reaches of the Heihe River Basin in Northwestern China. Observation data from three stations of the Watershed Allied Telemetry Experimental Research (WATER) program were used to validate the coupled models. The results are analyzed in Sect. 4, and conclusions are provided in Sect. 5.

2 Model development

The critical part of the coupling of GWM and LSM is the soil moisture movement in the vadose zone, which is simulated in both models. If the vadose zone water movement in the two models can be linked and integrated, a water cycle process can be completely simulated. In our study, a GWM called AquiferFlow that can simulate water movement in saturated and unsaturated zones (Wang, 2007; Wang et al., 2010), one LSM model, SiB2, which is used to simulate the water and energy movement above the ground surface and soil moisture movement in the subsurface up to three layers, were chosen as the base model to coupling. Based on the structures of the two models, their coupling is achieved by replacing the three-layer soil moisture simulation in the SiB2 code by the unsaturated zone water movement simulation of AquiferFlow. The principle of these two models and their coupling scheme are presented in detail in the following.

HESSD
9, 1163–1205, 2012

2.1 AquiferFlow

AquiferFlow (Wang, 2007; Wang et al., 2010) is a typical numerical GWM in which rectangular grid cells are used to divide the simulation domain, and the finite difference method (FDM) is used to solve groundwater movement equations in saturated and unsaturated zones. The main feature of AquiferFlow is that the conceptual model is similar to traditional saturated GWMs with block-centered FDM, but the Richard equation is fully incorporated to deal with unsaturated flow, as follows:

$$\frac{\partial}{\partial x}\left(K_{xx}K_{\mathrm{r}}\frac{\partial H}{\partial x}\right)+\frac{\partial}{\partial y}\left(K_{yy}K_{\mathrm{r}}\frac{\partial H}{\partial y}\right)+\frac{\partial}{\partial z}\left(K_{zz}K_{\mathrm{r}}\frac{\partial H}{\partial z}\right)+\varepsilon=S_{\mathrm{s}}\frac{\partial H}{\partial t} \quad (1)$$

where x, y and z are coordinates (m) in which z is oriented positively upward, and H is the hydraulic head (m) defined as $H=z_{\mathrm{g}}+\psi$, where ψ is the water suction potential of unsaturated soil (m), and z_{g} is the saturated groundwater table height (m), K_{xx}, K_{yy} and K_{zz} are the saturation hydraulic conductivity along the x,y and z directions ($\mathrm{m\,s^{-1}}$), respectively; K_{r} is the relative hydraulic conductivity, defined as a fraction of unsaturated conductivity and saturated conductivity; S_{s} is the extended specific storage and can be used in the saturated and unsaturated zones ($\mathrm{m^{-1}}$); ε is the source and sink term ($\mathrm{s^{-1}}$); and t is the time (s). Compared with the traditional governing equation of saturated groundwater, Eq. (1) introduces new parameters, namely, relative hydraulic conductivity (K_{r}) and an extension of the specific storage (S_{s}) for the calculation of water movement in an unsaturated zone. The relative hydraulic conductivity is a function of the pressure head. In AquiferFlow, Gardner and Fireman's method (1958) is used to relate K_{r} to soil moisture potential, ψ.

$$K_{\mathrm{r}}=\exp(-C_k\psi),\quad \psi<\psi_{\mathrm{s}};\quad K_{\mathrm{r}}=1,\quad \psi\geq\psi_{\mathrm{s}} \quad (2)$$

where C_k is the attenuation coefficient of permeability ($\mathrm{m^{-1}}$), and ψ_{s} is the saturation moisture potential (m). The specific storage is defined as the different forms in the saturated ($\psi\geq\psi_{\mathrm{s}}$) and unsaturated ($\psi<\psi_{\mathrm{s}}$) conditions. The specific storage depends

HESSD
9, 1163–1205, 2012

on the compressibility of the porous media and water in the saturated zone and is a function of soil volumetric water content (θ) ($m^3\,m^{-3}$) and soil moisture potential (ψ) in the unsaturated zone.

$$S_s = C_s(\psi) = -\frac{d\theta}{d\psi}, \quad \psi < \psi_s \tag{3a}$$

$$S_s = \rho_w g(\alpha + \phi\beta), \quad \psi \geq \psi_s \tag{3b}$$

where C_s is the specific moisture capacity (m^{-1}); ρ_w is the water density ($kg\,m^{-3}$); α is the coefficient of soil compressibility ($kg^{-1}\,m\,s^2$); β is the coefficient of groundwater compressibility ($kg^{-1}\,m\,s^2$); ϕ is the porosity; and g is the gravity acceleration ($m\,s^{-2}$).

The relationship between soil moisture potential, ψ, and the moisture content, θ, in the aquifer media is described by the suction curve, $\theta(\psi)$. In AquiferFlow, the suction curve can be created with the commonly used van Genuchten's (1980) equation or a simple exponential equation as

$$S_e = \frac{\theta - \theta_r}{\phi - \theta_r} = \exp(-C_w\psi), \quad \psi < \psi_s; \quad S_e = 1, \quad \psi \geq \psi_s \tag{4}$$

where S_e is the effective saturation; θ_r is the residual saturation; and C_w is the attenuation coefficient of soil moisture (m^{-1}) and an empirical parameter.

The equations of AquiferFlow are based on the groundwater dynamics principle; thus, it can describe water movement not only in the saturated zone but also in the unsaturated zone (Wang et al., 2010). However, the ET simulation in AquiferFlow, similar to most existing GWMs, is treated as a sink term for the groundwater system, and the ET calculation depends only on the soil moisture of the top soil layer and the potential ET of the location. Obviously, the ET simulation in AquiferFlow is empirical and is unable to represent a complex physical process. In summary, the governing equations of the GWMs are derived from the water conservation and do not include the simulation of energy and the biological processes. The water phase change process of evaporation and the vegetation root uptake process of transpiration are usually simplified in

HESSD
9, 1163–1205, 2012

the parameterization scheme of GWMs, and therefore, a model that can simulate the energy cycle and the biological processes, such as an LSM, needs to be coupled with GWMs to overcome this weakness.

2.2 SiB2

The simple biosphere model (SiB) (Sellers et al., 1986) is a typical land surface model that can be used to calculate the transfer of energy, mass, and momentum between the atmosphere and the vegetated surface of the Earth. Sellers et al. (1996b) produced a new version of the model, SiB2, by improving the hydrological sub-model, increasing the canopy photosynthesis-conductance model and introducing snowmelt process simulation into the SiB. After the release of the SiB, the model was verified and applied in many case studies (Vidale and Stockli, 2005; Sen et al., 2000; Sellers et al., 1989; Gao et al., 2004; Colello et al., 1998; Baker et al., 2003; Li and Koike, 2003). The study results indicated that the model could provide an adequate description of the energy and water processes above the ground surface.

In the model structure, the SiB2 is divided into five layers in the vertical direction: one vegetation layer, one ground layer above the ground surface, and three layers below the ground surface that represent the surface soil layer, the root layer, and the deep soil layer. The ground vegetation is classified into 9 types to represent various global vegetation conditions. The main inputs of the model include meteorological data, soil data, and the morphological, physiological, and biophysical parameters of vegetation. For the purpose of coupling, we only provide a detailed description of the soil moisture movement and evaporation processes; the other processes can be found in the relevant literature (Sellers et al., 1986, 1989, 1996a,b).

In the SiB2, precipitation reaches the ground surface after the canopy interception, and some water infiltrates to the subsurface limited by the local soil infiltration capacity. If the residual precipitation still exceeds the ground water storage capacity, runoff is generated. This process can be expressed as

HESSD
9, 1163–1205, 2012

$$R_0 = P_g - Q_1 - E_{gi} \quad (5)$$

where R_0 is runoff ($m\,s^{-1}$); P_g is the precipitation reaching the ground surface ($m\,s^{-1}$); Q_1 is the infiltrated water from the ground surface to the first soil layer ($m\,s^{-1}$); and E_{gi} is the evaporation from the interception of the ground surface ($m\,s^{-1}$).

As the water infiltrates into the soil, the water balance in the three soil layers is defined as

$$\frac{\partial W_1}{\partial t} = \left[Q_1 - Q_{12} - E_{gs}/\rho_w\right]/\theta_s D_1 \quad (6a)$$

$$\frac{\partial W_2}{\partial t} = \left[Q_{12} - Q_{23} - E_{ct}\rho_w\right]/\theta_s D_2 \quad (6b)$$

$$\frac{\partial W_3}{\partial t} = \left[Q_{23} - Q_3\right]/\theta_s D_3 \quad (6c)$$

where W_i is the wetness in the i-th layer, and $W_i = \theta_i/\theta_s$, θ_i is the volumetric soil moisture content in the i-th layer; θ_s is the volumetric soil moisture content for the saturation condition; E_{gs} is the evaporation from the surface soil layer ($m\,s^{-1}$); E_{ct} is the vegetation canopy transpiration ($m\,s^{-1}$); $Q_{i,i+1}$ is the water exchange between the i and $i+1$ layers ($m\,s^{-1}$); Q_3 is the base flow that drains out from the bottom of the soil ($m\,s^{-1}$); and D_i is the thickness of the i-th layer (m).

The moisture movement between the soil layers is described by Richard's equation, and the unsaturated zone hydraulic conductivity K ($m\,s^{-1}$) and soil moisture potential ψ (m) are calculated using the scheme of Clapp and Hornberger (1978), which is a function of soil wetness (W).

$$K = K_s W_i^{(2B+3)} \quad (7)$$

$$\psi = \psi_s W_i^{-B} \quad (8)$$

HESSD
9, 1163–1205, 2012

where K_s is the saturation hydraulic conductivity ($m\,s^{-1}$), ψ_s is the saturation moisture potential (m), and B is an empirical parameter. K_s, ψ_s and B are dependent on the soil characteristics and can be obtained from the empirical equations, which are defined as the function of soil texture (Yang et al., 2005; Cosby et al., 1984).

The ET processes in SiB2 consist of four parts: vegetation canopy transpiration (E_{ct}), evaporation from the interception of the canopy (E_{ci}), evaporation from the interception of the ground (E_{gi}) and evaporation from the surface soil layer (E_{gs}). The calculation of ET uses the electrical analog scheme, and the ET, denoted as the latent heat flux, is equal to the vapor pressure difference divided by the resistances among the different simulation points. The formulas are as follows:

$$\lambda E_{ct} = \left[\frac{e^*(T) - e_a}{1/g_c + 2r_b}\right]\frac{\rho c_p}{\gamma}(1 - W_c) \tag{9a}$$

$$\lambda E_{ci} = \left[\frac{e^*(T) - e_a}{r_b}\right]\frac{\rho c_p}{\gamma}W_c \tag{9b}$$

$$\lambda E_{gi} = \left[\frac{e^*(T) - e_a}{r_d}\right]\frac{\rho c_p}{\gamma}W_g \tag{9c}$$

$$\lambda E_{gs} = \left[\frac{h_{soil}e^*(T) - e_a}{r_{soil} + r_d}\right]\frac{\rho c_p}{\gamma}(1 - W_g) \tag{9d}$$

where λ is the latent heat of vaporization ($J\,kg^{-1}$); λE is the latent heat deduced from the ET ($W\,m^{-2}$); $e^*(T)$ is the saturated vapor pressure at temperature T (Pa); e_a is the canopy air space vapor pressure (Pa); ρ is the density of air ($kg\,m^{-3}$); c_p is the specific heat of air ($J\,kg^{-1}\,K^{-1}$); γ is the psychrometric constant ($Pa\,K^{-1}$); W_c is the fractional wetted area of the canopy; W_g is the fractional wetted area of the ground surface; g_c is the canopy conductance ($m\,s^{-1}$), a parameter associated with the biological process and vegetation growth environment (e.g. water potential of the root zone, temperature); r_b is the bulk canopy boundary layer resistance ($s\,m^{-1}$), which is a function of the

HESSD
9, 1163–1205, 2012

wind speed, temperature, canopy structure and other factors and is considered as an energy-related parameter; r_d is aerodynamic resistance between the ground and canopy air space ($s\,m^{-1}$), which is related to wind speed, ground surface roughness, and other factors; h_{soil} is the relative humidity of the soil pore space; and r_{soil} is the soil surface resistance ($s\,m^{-1}$), representing the impact of soil to the water vapor diffusion.

It can be seen from the above description that the ET simulation in the SiB2 is based on the physical mechanism, in which the impacts of water, energy and biological processes are all considered. However, in the SiB2, the description of water movement in the subsurface is relatively simple, and the soil water movement is limited to a shallow depth of an unsaturated zone; the GWT and lateral flow are not considered in the model. Additionally, precipitation as the single source term of the model cannot reflect the real situation of the water cycle on a watershed scale. The simulation errors from the water cycle will eventually cause errors in the energy cycle calculation and the biological process simulation. Coupling the LSM and GWM will be a good approach toward improving the simulated accuracy of the model.

2.3 Coupled model approach

As aforementioned, the SiB2 and AquiferFlow have their strengths and weaknesses. Coupling the two models can overcome their weaknesses and more accurately simulate the water and energy cycles. In the study presented here, the two models were tightly coupled from the model codes, and a new model, named GWSiB, was developed. We will introduce the coupling method from the mechanism in the following section.

In the coupled model, SiB2 simulates the energy balance, vegetation root water uptake and hydrologic processes above the ground surface, and AquiferFlow simulates water movement in the subsurface, including in the saturated and unsaturated zones. In detail, SiB2 is used to calculate the precipitation infiltration (Q_1), moisture

HESSD
9, 1163–1205, 2012

evaporation (E_{gs}) and transpiration (E_{ct}) based on the energy balance and the mass balance. The calculated results are used as the sink/sources (ε) and are input into AquiferFlow to calculate the groundwater potential (ψ). The obtained water potential is then used to calculate the groundwater movement in the model grids. The obtained new groundwater condition is eventually transferred back to the SiB2 to complete the calculation cycle in one time step. A flowchart of the coupling procedure is illustrated in Fig. 1.

The coupling of the two models includes spatial and temporal coupling. First, we discuss coupling the two models in space. From the model structure, the SiB2, a vertical one-dimensional model, must be extended horizontally to match AquiferFlow, a three-dimensional model. In our study, the mesh of the coupled model uses the AquiferFlow scheme in the horizontal, which means that on every topmost cell of the AquiferFlow grid, an SiB2 simulation is built. In the vertical space, AquiferFlow has a more flexible layer than SiB2; thus, the three subsurface layers in SiB2 are preserved, and the three top layers in AquiferFlow are set consistent with them. The infiltration and soil evaporation are linked with the top layer of AquiferFlow, and the root zone uptake is linked with the second layer.

It is noted that although the runoff (R_0) and base flow (Q_3) have been calculated on a vertical column in the SiB2, the water convergence between cells is not taken into account in the coupled model. This simplification will not cause a significant deviation when the model is used in the middle or lower reaches of an arid and semi-arid basin because there are almost no flow confluence processes in these regions. However, if the model is used in the upper reaches of a basin, the errors will not be ignored. Wang et al. (2009) studied this problem through coupling SiB2 with a geomorphology-based hydrological model (GBHM). In our study, the middle reaches of the Heihe River Basin are selected as the study areas. Runoff is not the key hydrological process in this region; thus, the coupled model can be used here.

We now discuss how to handle the temporal discretization of the coupled models. LSMs usually use a time step of one hour or less because the variables of energy

HESSD
9, 1163–1205, 2012

and mass simulated by the LSM vary rapidly, such as the soil surface temperature, and they vary significantly from day to night. However, the groundwater head and flow vary more slowly; thus, the time intervals in GWMs are usually one day or longer. LSMs are more sensitive to time resolution than GWMs, which generally cannot accept time intervals greater than one hour. Assuming the time step in LSMs is one day, the temporal fluctuations in hours will smooth out, generating significant calculation errors and even making the simulation meaningless. A shorter time interval will not significantly affect the simulation accuracy in GWMs but will significantly reduce its computational efficiency.

Considering the time steps used in the two models, two optional time coupling schemes are implemented in the coupled model. One is the time step used in AquiferFlow (the same as that in SiB2), which is set to be either one hour or 30 min. Another scheme is that in AquiferFlow, where the time step is adopted as one day, which is normally used in the code, while the time step in SiB2 is one hour. The fluxes of SiB2 are accumulated in one day and are then exchanged with AquiferFlow. The first scheme has higher precision and more computation; thus, it is suitable for theoretical analysis or small-scale simulation. The second scheme greatly improves the computational efficiency and achieves acceptable calculation accuracy. This scheme is more suitable for large area simulation.

Because different unsaturation soil equations are used in AquiferFlow and SiB2, there is a discontinuity of soil moisture at the two model communication times, especially when using the second scheme, in which the accumulation of water is exchanged between GWM and LSM. To solve this problem, Clapp and Hornberger's (1978) soil moisture scheme used in SiB2 is introduced into the AquiferFlow model frame. In AquiferFlow, relative permeability (K_r) and effective saturation (S_e) are the two key parameters for soil moisture movement and content. These two parameters are defined as fractions in AquiferFlow and are used to control the moisture movement in the unsaturated zone by adjusting the saturated hydraulic conductivity (K_s) and saturated soil water content (θ_s), which is approximately equal to the porosity (ϕ). Meanwhile,

HESSD
9, 1163–1205, 2012

the parameters used in Clapp and Hornberger's (1978) soil moisture scheme are also based on the saturated moisture potential (ψ_s) and saturated hydraulic conductivity (K_s); thus, these equations can be transferred to the AquiferFlow form as:

$$S_e = W = \left(\frac{\psi_s}{\psi}\right)^{\frac{1}{B}} \tag{10}$$

$$K_r = \left(\frac{\psi_s}{\psi}\right)^{\frac{2B+3}{B}} \tag{11}$$

Replacing the K_r and S_e of the AquiferFlow model by Eqs. (2) and (4) makes the vadose zone parameters of AquiferFlow consistent with the SiB2 and reduces the soil moisture discontinuities of the model at the time of coupling.

After the GWSiB model is built, it is applied to the middle reaches of the Heihe River Basin, which is a typical arid and semi-arid region of Western China, to test its effectiveness and applicability. Field observations from three point locations and an entire study area are used to validate the developed model. The following sections will detail the model validation.

3 Case study

3.1 Study area

For the validation of the model, a case study was undertaken in the middle reaches of the Heihe River Basin, which is an arid inland river basin located in Northwestern China. A comprehensive field experiment titled the Watershed Allied Telemetry Experimental Research (WATER) project was conducted in 2008 in this basin. This project aimed to improve the observability, understanding, and predictability of hydrological and related ecological processes at a catchment scale. In the experiment, an intensive

HESSD
9, 1163–1205, 2012

observation period lasted from 20 May to 21 August 2008, and some automatic meteorological stations (AMSs) were installed for one-year observations or longer (Li et al., 2009). Numerous data types, such as soil moisture, radiation fluxes (shortwave and longwave radiation), latent heat (evapotranspiration), and sensible heat fluxes, were measured. These data provided the dataset for model validation in our study.

The middle reaches of the Heihe River Basin, a major part of the oasis in the Heihe plain, was selected as the study area in this paper. The latitude ranges from 38.7° N to 39.8° N, the longitude ranges from 98.5° E to 102° E, and the total area is approximately 10 000 km^2 (Fig. 2). Irrigated agriculture, grassland/steppe, wetland, and gobi are main land cover types of the study area. The study area, as an integral groundwater cell, is hydrogeologically referred to as the Zhangye Basin, and some groundwater numerical simulation work has been performed in this area, such as by Wen et al. (2007) and Su (2005), who used the FEFLOW model to simulate the groundwater movement of this area and forecasted the future groundwater change trends. Hu et al. (2007) developed a three-dimensional GWM and used it to study the groundwater interaction with rivers and springs in this area. Ding et al. (2009) developed a two-dimensional numerical model to simulate the groundwater dynamics of this area. Zhou et al. (2011) built a GWM of this area to quantify the effects of land use and anthropogenic activities on the groundwater system. These groundwater modeling studies provide an excellent reference.

3.2 Model settings

The study area is uniformly discretized into 79 rows and 32 columns horizontally, and each numerical cell has a dimension of 3 km × 3 km. In the vertical direction, the study area is discretized into 6 layers. The upper three layers are set to 0.02 m, 0.48 m, and 1.5 m, values that are consistent with the SiB2 soil layers and that represent the surface soil, the soil root, and deeper soil layers, respectively. The lower three layers are used to describe the hydrogeologic structure in the study area, and they represent the unconfined aquifer, the aquitard and the confined aquifer. The thicknesses of the

HESSD
9, 1163–1205, 2012

lower three layers are determined by the interpretation of the logging data obtained from 108 boreholes in the region, as proposed by Zhou et al. (1990). The study area contains a total of 106 179 ($79 \times 32 \times 6$) cells, as shown in Fig. 2.

For the initialization, a 90-m resolution digital elevation model (DEM) data obtained from the SRTM (Shuttle Radar Topography Mission) are upscaled to 3 km to represent the topography of the study areas. The initial GWT distribution in the study area is obtained by the interpolation of GWT measurements conducted in December 2003 from 36 observation wells in the study area. Any GWT positions not available from the measurements are determined by the relevant literature (Zhou et al., 2011; Wen et al., 2007; Su, 2005; Hu et al., 2007). From the initial GWT (Fig. 2), it can be found that the main direction of groundwater of the middle reaches of the Heihe River Basin is from south to north and is roughly consistent with the surface river direction. The lower GWT is located in the north of the study area, where the groundwater discharges to the surface river. The boundary conditions and saturated hydraulic conductivity of the model were initially assigned with values according to previous study results in the Heihe River Basin (Zhou et al., 2011; Wen et al., 2007; Su, 2005; Hu et al., 2007; Ding et al., 2009). Later, these parameters were optimized through trial-and-error calculations, according to the GWT data obtained in January 2008. Ultimately, the boundary conditions of the model are set as fixed flow conditions: the southern boundary has 2360×10^4 m^3 water inflow every year, the northern boundary has 540×10^4 m^3 water inflow, and the western and eastern boundaries have a total of 120×10^4 m^3 water inflow. These water inflows were allocated to each of the active cells of the boundary grid on average in the model. The saturated hydraulic conductivity (K_s) field in the study area was divided into 24 sub-regions, with values ranging from 0.5 m d^{-1} to 20 m d^{-1}. The distribution of specific storage (S_s) was represented by 10 sub-regions, with values ranging from 0.003 m^{-1} to 0.17 m^{-1}. The water potential parameters of the unsaturated zone were determined according to the soil texture. The parameter values for the soil characteristics used in this study were obtained through analysis of the Chinese dataset of 1-km resolution multi-layer soil particle-size distribution (Shangguan et al., 2011).

HESSD
9, 1163–1205, 2012

The atmospheric data used in the model, including incident solar radiation, incident longwave radiation, wind speed, air pressure, vapor pressure, air temperature, and precipitation, are taken from the Global Land Data Assimilation System (GLDAS) project (Rodell et al., 2004). The spatial resolution of the original data is 25 km, and the temporal resolution is 3 h. The data are interpolated to a spatial resolution of 3 km and a temporal resolution of 1 h to fit the resolution of the coupled model. A statistical method provided by the Global Soil Wetness Project 2 (GSWP2) (for precipitation data) and the cubic spline method (Dai et al., 2003) (for other data) are used for the temporal interpolations of the data. The high-resolution meteorological interpolation model MicroMet (Liston and Elder, 2006) is used in the spatial interpolation of the data. These data are used in all of the model cells except those where AMSs are located. In those cells, the interpolated atmospheric data are replaced by the observation data.

The land cover data used in the model are derived from the Multi-source Integrated Chinese Land Cover (MICL Cover) (Ran et al., 2010). The International Geosphere-Biosphere Programme (IGBP) land cover classification system is used in the MICL Cover, and the land surface is classified into 18 types. In this study, the 18 types are grouped to nine types depending on the vegetation classification of SiB2 (Sellers et al., 1996b).

The time-dependent vegetation parameters used in the coupled model were obtained from the satellite data. The level-4 combined (Terra and Aqua) MODIS global LAI and FPAR products (MCD15A3), which are composited every 4 days at a resolution of 1 km, are linearly interpolated to a temporal scale of 1 h and are resampled to a spatial resolution of 3 km for the coupled model.

Taking into account the scope of the study area and the quantity of the cells, there is an enormous computation burden in the simulation. Therefore, the second scheme of time coupling is selected in our case study, which means an hourly time step is used in the SiB2 model and a daily time step is adopted in AquiferFlow. At the start time of each day, the two models exchange their values.

HESSD
9, 1163–1205, 2012

For the validation data, the full year of 2008 is selected as a simulation period. Because of the uncertainty of the initial conditions, which are based on the data of December 2003, the model is run four years for calibration. The simulated values at the last time (1 January 2008) of the calibration period are treated as the initial conditions of the coupled model.

4 Model validation and result analysis

The energy budget and water movement in the middle reaches of the Heihe River Basin were simulated from 1 January to 31 December 2008, using the coupled model. To validate the model, the simulated GWTs of the coupled model are compared with the observed GWTs, which are obtained from the interpolation of the 36 observation wells for GWT in December 2008; the results are shown in Fig. 2.

From the GWT comparison (Fig. 2), the simulation results and observations agree well except at the west and east sides of study area, where the groundwater depth is greater than 100 m and there are usually no groundwater observation wells. The initial GWTs of these regions are taken from values from the existing literature (Wen et al., 2007; Su, 2005). The validation values of the model in the region were derived from the extrapolation of 36 observation wells. We believe the uncertainties of the GWTs in these areas are the main reason for the simulation errors. In addition, at the upper section of the Heihe River, the simulated GWTs are higher than the observed GWTs (e.g. the 1450 m GWT) in Fig. 2 due to the upper section of the Heihe River being considered as the region of surface water recharge to the groundwater in the coupled model. The intense water infiltration of this region and the partial GWT increase are simulated in the model, but this change cannot be represented in the observation because the observed wells are limited in these regions for the GWT interpolation.

In addition, the ET and soil moisture observations of the three stations in the study area are compared with the model simulations. The three stations include two AMSs, the Linze grassland station (LZG) and the Yingke oasis station (YK) in the WATER

HESSD
9, 1163–1205, 2012

project, and one normal meteorological station, the National Observatory on Climatology at Zhangye (ZYNOC). A groundwater depth map obtained by the kriging interpolation based on the average GWT in December 2008 and a digital elevation model (DEM) of this region (Fig. 3) are used to locate the spots of the three stations and to describe their geographic characteristics. Kollet and Maxwell (2008) indicated that 5 m is a critical depth at which the GWT is strongly correlated with ET. Thus, 5 m was set as the boundaries of the shallow groundwater zone in our study (Fig. 3). According to this depth limitation, the LZG station is located in the shallow groundwater zones, the YK and ZYNOC stations are located in the deeper groundwater zones, and the YK station is located in irrigated farmland. The groundwater below the YK would be affected by the irrigation processes. These three stations represent the typical water and energy cycles in the study area, and their detailed information is listed in Table 1. Figure 3 also shows that the shallow groundwater zones are mainly distributed along the Heihe River, while another is located in the Yanchi-Minghua area, which is the water collection zone of the Fengle and Maying Rivers. The compared results of these three stations are described in detail in the following sections.

4.1 Validation of the model at the Linze grassland station

The land covers at the Linze grassland station (LZG) are mainly wetland, grassland and salinized meadow. There is an AMS system in the LZG, which was used for observations from 1 October 2007 to 27 October 2008. The AMS system can provide all the necessary atmospheric forcing data for our modeling study. There is no direct measurement of latent heat from the LZG station, but it can be obtained from the sensible heat by the energy balance equation:

$$LE = R_n - H - G \tag{12}$$

where LE is latent heat ($W\,m^{-2}$); L is the heat of vaporization ($J\,kg^{-1}$); E is the evapotranspiration (m); R_n is the net radiation ($W\,m^{-2}$), equal to the difference of the downward radiation and the upward radiation, which can be obtain from the atmospheric

HESSD
9, 1163–1205, 2012

forcing data; and H is the sensible heat. In the WATER experiment period, a large aperture scintillometer (LAS) flux system was used to obtain the sensible heat data from 19 May 2008 to 20 July 2008, so that it could provide the sensible heat data for model; G is the ground heat flux (W m^{-2}) and is assumed to be proportional to the net radiation (Su, 2002),

$$G = R_n \cdot [\Gamma_c + (1 - f_c) \cdot (\Gamma_s - \Gamma_c)] \quad (13)$$

where $\Gamma_c = 0.05$ for a full vegetation canopy, $\Gamma_s = 0.315$ for bare soil, and f_c is the fractional canopy coverage, which is set to 0.81 in the LZG. The latent heat of the LZG is calculated according to a variety of observational data and the energy balance equation; then, the ET are deduced based on the latent heat.

Sixteen soil profiles at the LZG were chosen for soil moisture measurement. In each profile, the soil moisture was measured through probes at six soil layers, which were located below the surface at 10, 20, 30, 40, 60 and 100 cm from 31 May 2008 to 13 July 2008. The average of the 16 profile measurements is linearly interpolated to obtain the soil moisture distribution at LZG and the soil wetness (W) values, which are a fraction of the volumetric and saturated volumetric water contents. In Fig. 4, the soil wetness values obtained from the measurements are compared with the simulation results at the model's second and third layers.

Figure 4 shows that the soil moisture simulations from the coupled model, GWSiB, are higher than the results from the uncoupled model, SiB2, but closer to the measurements. It is shown from the GWSiB simulation results that the third layer's soil moistures from the coupled model are almost saturated, and the mean soil wetness of the second layer reaches 0.95. These results are consistent with the actual soil conditions in the LZG. However, the soil wetness values calculated from the two layers by the SiB2 are only 0.38 and 0.39, respectively, which are far from the measurements. Furthermore, the GWSiB simulation could provide a more stable relationship between precipitation and soil moisture than the SiB2 simulation because the groundwater converges at this region due to the lateral flow, which provides the water to the soil near

HESSD
9, 1163–1205, 2012

the ground surface by capillary action, maintaining the soil moisture and making it less sensitive to precipitation.

In Fig. 5, the measured ET at the LZG from 19 May 2008 to 27 August 2008, obtained by the energy balance equation, was compared with the simulated ET through the GWSiB and SiB2 in same period of time. It is shown from the figure that the SiB2 underestimates the ET. In the validation period, the diurnal variation of the observed ET is large, with values mainly between 3 mm to 6 mm. The average measured ET during the validation period is 3.93 mm, and the calculated results by the SiB2 and GWSiB are 1.16 mm and 3.66 mm, respectively. Obviously, GWSiB's simulation results are much better than SiB2's. This result is also confirmed by the statistical analysis of the absolute error and the relative error. The mean absolute error (MAE) of the ET simulated by GWSiB is 0.27 mm and that simulated by SiB2 is 2.50 mm. The mean relative errors (MRE) of the simulated ET by GWSiB and SiB2 are 6.8 % and 63.6 %, respectively. The reason GWSiB can provide a more realistic simulation than SiB2 is that the lateral flow of groundwater is taken into account in GWSiB, but not in SiB2. The lateral flow makes the groundwater accumulation in the shallow water region, and the saturated groundwater can supply water to the soil near the ground surface by the capillary action, which leads to a higher land surface soil moisture that is less sensitive to precipitation. Compared with the GWSiB, the SiB2 is a vertical one-dimensional model and cannot describe lateral water movement; consequently, the soil water moisture of the land surface is underestimated, and the lower soil moisture restricts the ET.

4.2 Validation of the model at the national observatory on climatology at Zhangye

The National Observatory on Climatology at Zhangye (ZYNOC) is one of China's national climatology stations. The station is located in the middle reaches of the Heihe River Basin, where the landscape is the gobi and the GWT is deep. Comprehensive atmospheric data, five layers of soil moisture data and heat flux were observed here. In

HESSD
9, 1163–1205, 2012

this study, data from 1 July 2008 to 30 September 2008 were obtained from the WATER and provided by the Gansu Provincial Meteorological Bureau. Some of these data are removed because of the data quality, and only 61 days of soil moisture observations and 45 days of latent heat observations were used for the model validation.

The observed soil moistures are linearly interpolated to their values at depths of 26 cm and 125 cm from the five-layer soil moisture observations at ZYNOC and are compared with the model simulations in Fig. 6. The soil moisture at the ZYNOC is highly sensitive to precipitation. The moisture content change has an approximately 1 day lag to the precipitation for the second layer and an approximately 2 day lag for the third layer. In comparison with the soil moistures in the two layers, the fluctuation of the second layer is more intensive than the third layer. Both GWSiB and SiB2 can depict this phenomenon. From the comparison between the simulation and the observation, the simulations of these two models agree well with the observation for the trends and magnitudes. If we compare the two model results, there are no significant differences between them. From the statistical analysis of the results, the MAE values of the two layers of soil wetness by GWSiB are 0.01 and 0.01, respectively, and their values by SiB2 are 0.009 and 0.007, respectively. The MRE values of the two soil wetness layers simulated by GWSiB are 2.9 % and 2.22 % and those simulated by SiB2 are 2.7 % and 1.6 %, respectively.

In Fig. 7, the simulation results of ET from GWSiB and SiB2 are compared with the observations at the ZYNOC. The simulated trends of the two models agree well with the observations, but the simulated magnitudes are slightly larger than the observations, especially in the low value zone, probably due to the uncertainty of the land surface vegetation parameters, such as the vegetation types, which have only 9 defined types in SiB2. Additionally, "broadleaf shrubs with bare soil" is the closest vegetation type to the ZYNOC, but it still cannot fully describe the land surface conditions at the ZYNOC. The vegetation coverage, grid scale, and other factors also contribute to the error. For the ET data analysis, the MAEs of GWSiB and SiB are 0.4 mm and 0.2 mm, respectively, and the MREs are 35.4 % and 15.4 %, respectively. It should be noted that the

HESSD
9, 1163–1205, 2012

observation data from 14 August 2008 to 18 September 2008 are missing, which can affect the results of the statistical analysis.

4.3 Validation of the model at the Yingke oasis station (YK)

The Yingke (YK) oasis station is located in a typical irrigated farmland. Maize and wheat are the main crops here. The groundwater depth of this location is approximately 71.7 m, and the saturated groundwater hardly affects the surface soil layers, but the irrigation process can directly increase the subsurface water content. In the WATER experiment, an AMS is established in YK, and normal atmospheric data and 6 layers of soil moistures at 0.1 m, 0.20 m, 0.40 m, 0.80 m, 1.20 m, and 1.60 m depths were observed. In addition, an eddy covariance system (EC) is used to observe the latent heat. All these factors were continuously observed from 1 January 2008 to the present. The majority of the data are of good quality, although some data are not available. In this study, a crop growth period, 1 April 2008 to 1 October 2008, was chosen as the model validation period.

Because GWSiB has a groundwater sub-model, it can be used to simulate an irrigation infiltration process and soil moisture variation; however, the SiB2 cannot because there is no corresponding module in the model.

The soil wetness data interpolated to 26 cm and 125 cm from the YK soil moisture observation, the precipitation data, the irrigation data and the two-layer soil wetness of the model simulation are shown in Fig. 8. This figure shows that irrigation is the most important factor in soil moisture variation. In the entire validation period, the cumulative amount of irrigation is 342 mm, while the precipitation is only 117 mm. Comparing the two models, GWSiB can better describe the change of soil moisture that is affected by the irrigation process, and its calculations for the soil wetness are in good agreement with the observations, while the SiB2 obviously underestimated the soil moisture because the irrigation process is not considered. The average soil wetness of observations with the two layers in the validation period are 0.75 and 0.86. The soil wetness values calculated by GWSiB are 0.66 and 0.91, respectively, and those calculated by

HESSD
9, 1163–1205, 2012

SiB2 are 0.29 and 0.31, respectively. The differences between the coupled and uncoupled models can also be reflected from their calculated MAE and MRE results for soil wetness. The MAEs of the two-layer soil wetness simulated by GWSiB are 0.09 and 0.05, and those simulated by SiB2 model are 0.46 and 0.55, respectively. The MREs of the two-layer soil wetness simulated by GWSiB are 12.0 % and 5.8 %, but those simulated by SiB2 are 61.3 % and 64.0 %.

Figure 9 is used to compare the simulated ET results from the two models with the observation at YK. This figure shows that the GWSiB model can well simulate the ET at YK in the trends and magnitudes, especially in the case of weak ET. In July and August, however, when the net radiation is the most intense in the year, the coupled model underestimates the ET by approximately 21 %. This problem is probably due to the coupling scheme adopted in the coupled model. In this study, a time step of one day was used in the groundwater simulation and a time step of one hour was used in the land surface simulation, and the two models exchange water only at the beginning of a day. (The details are shown in Sect. 2.) This led to the water of ground surface soil layer cannot be supply by the the deep groundwater in time, and this effect will be more obvious on the strong ET time. In contrast, the SiB2 gives a lower ET simulation than the GWSiB because additional soil water from the irrigation is not taken into account in it. From the data analysis, the MAE value of the simulated ET by GWSiB to the observation in the validation period is 0.39 mm per day, and the value for the SiB2 result is 2.43 mm per day. The MRE for the simulated ET of GWSiB is 11.5 %, and the MRE for the SiB2 is 71.9 %.

Obviously, the coupled model takes more physical processes, such as the irrigation processes, into account and can more realistically simulate the water cycle than the uncoupled model.

HESSD
9, 1163–1205, 2012

4.4 Analysis of regional evapotranspiration

The regional ET is an important factor in the regional water and energy balances. The GWSiB is a three-dimensional water and energy simulation model; thus, it has the ability to predict regional ET. In this study, the ET of the middle reaches of the Heihe River Basin was simulated by both the GWSiB and the SiB2 every hour in 2008, and the daily ET, which is the sum of the 24 hourly ET on 21 June 2008, is shown in Fig. 10. Because it is difficult to accurately measure the regional scale ET, we only analyze the rationality of the simulated regional ET, and we qualitatively compare the results with the exiting studies (Li and Zhao, 2010; Zhou et al., 2011).

Li and Zhao (2010) and Zhou et al. (2011) calculated the regional ET from instantaneous satellite data and upscaled them to a daily ET. Li and Zhao (2010) showed that the maximal ET values in the middle reaches of the Heihe River Basin were 3.28 mm on 23 September 2007 and that 27.4 % of the study area has greater than 2 mm of ET. Zhou et al.'s (2011) results indicate that the maximal ET value in this region is 8.13 mm, and the ET values in the Heihe River zones and irrigation areas were mostly between 4.07 mm and 5.4 mm on 10 July 2005. In our study, the simulated ET values by GWSiB range from 0.30 mm to 6.61 mm, and the simulated results by SiB2 range from 0.03 mm to 1.82 mm. Clearly, the calculated results by GWSiB are more consistent with the results of other studies than those calculated by SiB2. In addition, for the simulation results by GWSiB, the ET values are low in the northern part of the study area, with high values along the Heihe River, especially in the MingHua–YanChi wetland area and in irrigated agricultural areas. The obtained ET is positively correlated with the soil moisture distribution of the study area. In contrast, the ET results simulated by SiB2 are more even over the entire study area. These results also indicate that the results simulated by GWSiB are more reasonable than those simulated by SiB2 because the soil moisture always has a positive correlation with ET.

HESSD
9, 1163–1205, 2012

5 Summary and conclusions

The LSM can well describe the land surface energy and water cycles, but the water movement of the subsurface is oversimplified, and the lateral flow of groundwater is ignored. Conversely, the GWM can describe the dynamic movement of subsurface water, but it cannot simulate the physical mechanism of ET, which is an important component of the water cycle because this process involves the biochemical energy cycle and biological processes. Coupling the two models can effectively overcome their respective shortcomings, and by linking the energy and water cycles together, to simulate these processes more comprehensive and potentially more accurate.

In this study, a typical land surface model, SiB2, and a typical groundwater model, AquiferFlow, are fully coupled. In the coupling scheme, infiltration, evaporation and transpiration, which are simulated by the SiB2, are inputed into AquiferFlow, and the soil moistures calculated by the AquiferFlow are used in the SiB2. The coupled model then is applied to the middle reaches of the Heihe River Basin and is validated by the field observation of three stations representing the shallow groundwater depth region, the deep groundwater depth region and the irrigation region. From the simulation results of the shallow groundwater depth zone, the coupled model predicted a higher soil moisture and ET than the uncoupled model, and its results are closer to the observation than the uncoupled model. In the deeper groundwater zone, the performances of the coupled and uncoupled models are similar, and the simulated soil moisture and ET of the two models are in good agreement with the observed data in this region. In the irrigation area, the coupled model better captures the soil moisture and ET changes, which are affected by the irrigation process because irrigation is taken into account in the coupled model, but not in the uncoupled model. Additionally, in the regional ET analysis, the simulated results of the coupled model are more reasonable than those by SiB2 and exhibit a good positive correlation with the soil moisture distribution of the study area.

From our study, the following four conclusion can be obtained.

HESSD
9, 1163–1205, 2012

1. At the basin scale, the lateral flow of groundwater plays an important role in the water cycle, especially in the shallow groundwater depth zone, where it can significantly affect the water and energy cycle. If the groundwater lateral flow is ignored in this region, the subsurface soil moisture and land ET will be significantly underestimated.

2. The interaction of groundwater and the land surface process is weak in the deeper groundwater depth zone. The soil moisture of this region mainly comes from the precipitation, which is always considered as vertical movement. Thus, the one-dimensional LSM can capture the key processes of the water and energy cycle under these conditions.

3. Irrigation can strongly influence the water and energy processes of irrigated areas, and this effect is even greater than the effect of precipitation. Therefore, the irrigation process is appropriate to consider in the model and will greatly improve the simulation accuracy of the energy and water cycles in this region.

4. The SiB2, as a vertical one-dimensional LSM, is not suitable for use in the shallow groundwater depth zone or irrigation areas. The SiB2 model applied in these areas will result in underestimated soil moisture and ET. In contrast, the coupled model, which integrates the LSMs and GWMs, shows good performance in all cases. It not only improves the simulation accuracy but also the applicability, improving the water and energy cycle simulation.

Although the coupled model improves the water and energy cycle simulation over the uncoupled model, there are still some deficiencies. Surface water movement processes, such as surface water convergence, river water conveyance, and water resource allocation, being an important part of the water cycle, are not considered. The soil freezing and thawing processes, which are specific processes in cold regions, are also ignored in the model. Adding the above processes to the coupled model and continuing to improve its simulation accuracy will be the main direction of future studies.

HESSD
9, 1163–1205, 2012

Acknowledgement. This work is supported by the National Science Fund for Distinguished Young Scientists, "Development of a Catchment-Scale Land Data Assimilation System" (grant number: 40925004). The data used in the paper are obtained from the Watershed Allied Telemetry Experimental Research (http://westdc.westgis.ac.cn/water/).

References

Baker, I., Denning, A. S., Hanan, N., Prihodko, L., Uliasz, M., Vidale, P. L., Davis, K., and Bakwin, P.: Simulated and observed fluxes of sensible and latent heat and CO_2 at the WLEF-TV tower using SiB2.5, Global Change Biol., 9, 1262–1277, 2003.

Clapp, R. B. and Hornberger, G. M.: Empirical equations for some soil hydraulic properties, Water Resour. Res., 14, 601–604, doi:10.1029/WR014i004p00601, 1978.

Colello, G. D., Grivet, C., Sellers, P. J., and Berry, J. A.: Modeling of energy, water, and CO_2 flux in a temperate grassland ecosystem with SiB2: May–October 1987, J. Atmos. Sci., 55, 1141–1169, 1998.

Cosby, B. J., Hornberger, G. M., Clapp, R. B., and Ginn, T. R.: A statistical exploration of the relationships of soil-moisture characteristics to the physical-properties of soils, Water Resour. Res., 20, 682–690, 1984.

Dai, Y., Zeng, X., Dickinson, R. E., Baker, I., Bonan, G. B., Bosilovich, M. G., Denning, A. S., Dirmeyer, P. A., Houser, P. R., Niu, G., Oleson, K. W., Schlosser, C. A., and Yang, Z.-L.: The Common Land Model, B. Am. Meteorol. Soc., 84, 1013–1023, doi:10.1175/bams-84-8-1013, 2003.

Ding, H.-W., Xu, D.-L., Zhao, Y.-P., and Yang, J.-J.: Dynamic characteristic and forecast of spring water in the middle reaches of Heihe River trunk stream area in Gansu Province, Arid Land Geogr., 32, 726–732, 2009.

Fan, Y., Miguez-Macho, G., Weaver, C. P., Walko, R., and Robock, A.: Incorporating water table dynamics in climate modeling: 1. Water table observations and equilibrium water table simulations, J. Geophys. Res.-Atmos., 112, D10125, doi:10.1029/2006jd008111, 2007.

Gao, Z. Q., Chae, N., Kim, J., Hong, J. Y., Choi, T., and Lee, H.: Modeling of surface energy partitioning, surface temperature, and soil wetness in the Tibetan prairie using the Simple Biosphere Model 2 (SiB2), J. Geophys. Res.-Atmos., 109, D06102 doi:10.1029/2003jd004089, 2004.

HESSD

9, 1163–1205, 2012

Gardner, W. R. and Fireman, M.: Laboratory studies of evaporation from soil columns in the presence of a water table, Soil Sci., 85, 244–249, 1958.
Gedney, N. and Cox, P. M.: The sensitivity of global climate model simulations to the representation of soil moisture heterogeneity, J. Hydrometeorol., 4, 1265–1275, doi:10.1175/1525-7541(2003)004<1265:tsogcm>2.0.co;2, 2003.
Gutowski Jr., W. J., Vörösmarty, C. J., Person, M., Ötles, Z., Fekete, B., and York, J.: A Coupled Land-Atmosphere Simulation Program (CLASP): calibration and validation, J. Geophys. Res., 107, 4283, doi:10.1029/2001jd000392, 2002.
Holt, T. R., Niyogi, D., Chen, F., Manning, K., LeMone, M. A., and Qureshi, A.: Effect of land-atmosphere interactions on the IHOP 24–25 May 2002 convection case, Mon. Weather Rev., 134, 113–133, doi:10.1175/mwr3057.1, 2006.
Hu, L.-T., Chen, C.-X., Jiao, J. J., and Wang, Z.-J.: Simulated groundwater interaction with rivers and springs in the Heihe River Basin, Hydrol. Process., 21, 2794–2806, doi:10.1002/hyp.6497, 2007.
Kollet, S. J. and Maxwell, R. M.: Integrated surface-groundwater flow modeling: a free-surface overland flow boundary condition in a parallel groundwater flow model, Adv. Water Resour., 29, 945–958, doi:10.1016/j.advwatres.2005.08.006, 2006.
Kollet, S. J. and Maxwell, R. M.: Capturing the influence of groundwater dynamics on land surface processes using an integrated, distributed watershed model, Water Resour. Res., 44, W02402, doi:10.1029/2007wr006004, 2008.
Li, S. B. and Zhao, W. Z.: Satellite-based actual evapotranspiration estimation in the middle reach of the Heihe River Basin using the SEBAL method, Hydrol. Process., 24, 3337–3344, doi:10.1002/Hyp.7748, 2010.
Li, X. and Koike, T.: Frozen soil parameterization in SiB2 and its validation with GAME-Tibet observations, Cold Reg. Sci. Technol., 36, 165–182, 2003.
Li, X., Li, X. W., Li, Z. Y., Ma, M. G., Wang, J., Xiao, Q., Liu, Q., Che, T., Chen, E. X., Yan, G. J., Hu, Z. Y., Zhang, L. X., Chu, R. Z., Su, P. X., Liu, Q. H., Liu, S. M., Wang, J. D., Niu, Z., Chen, Y., Jin, R., Wang, W. Z., Ran, Y. H., Xin, X. Z., and Ren, H. Z.: Watershed allied telemetry experimental research, J. Geophys. Res.-Atmos., 114, D22103, doi:10.1029/2008jd011590, 2009.
Liang, X., Xie, Z. H., and Huang, M. Y.: A new parameterization for surface and groundwater interactions and its impact on water budgets with the variable infiltration capacity (VIC) land surface model, J. Geophys. Res.-Atmos., 108, 8613, doi:10.1029/2002jd003090, 2003.

HESSD
9, 1163–1205, 2012

Liston, G. E. and Elder, K.: A meteorological distribution system for high-resolution terrestrial modeling (MicroMet), J. Hydrometeorol., 7, 217–234, 2006.
Maxwell, R. M. and Miller, N. L.: Development of a coupled land surface and groundwater model, J. Hydrometeorol., 6, 233–247, doi:10.1175/jhm422.1, 2005.
Maxwell, R. M., Chow, F. K., and Kollet, S. J.: The groundwater-land-surface-atmosphere connection: soil moisture effects on the atmospheric boundary layer in fully-coupled simulations, Adv. Water Resour., 30, 2447–2466, doi:10.1016/j.advwatres.2007.05.018, 2007.
Maxwell, R. M., Lundquist, J. K., Mirocha, J. D., Smith, S. G., Woodward, C. S., and Tompson, A. F. B.: Development of a coupled groundwater-atmosphere model, Mon. Weather Rev., 139, 96–116, doi:10.1175/2010mwr3392.1, 2011.
McDonald, M. G. and Harbaugh, A. W.: A Modular Three-Dimensional Finite-Difference Ground-Water Flow Model, United States Geological Survey, US Government Printing Office, Washington, DC, 576 pp., 1988.
Niu, G. Y., Yang, Z. L., Dickinson, R. E., Gulden, L. E., and Su, H.: Development of a simple groundwater model for use in climate models and evaluation with gravity recovery and climate experiment data, J. Geophys. Res.-Atmos., 112, D07103, doi:10.1029/2006jd007522, 2007.
Ran, Y. H., Li, X., and Lu, L.: Evaluation of four remote sensing based land cover products over China, Int. J. Remote Sens., 31, 391–401, doi:10.1080/01431160902893451, 2010.
Rodell, M., Houser, P. R., Jambor, U., Gottschalck, J., Mitchell, K., Meng, C. J., Arsenault, K., Cosgrove, B., Radakovich, J., Bosilovich, M., Entin, J. K., Walker, J. P., Lohmann, D., and Toll, D.: The Global Land Data Assimilation System, B. Am. Meteorol. Soc., 85, 381–394, doi:10.1175/bams-85-3-381, 2004.
Sellers, P. J., Mintz, Y., Sud, Y. C., and Dalcher, A.: A simple biosphere model (sib) for use within general-circulation models, J. Atmos. Sci., 43, 505–531, 1986.
Sellers, P. J., Shuttleworth, W. J., Dorman, J. L., Dalcher, A., and Roberts, J. M.: Calibrating the simple biosphere model for amazonian tropical forest using field and remote-sensing data, 1. Average calibration with field data, J. Appl. Meteorol., 28, 727–759, 1989.
Sellers, P. J., Los, S. O., Tucker, C. J., Justice, C. O., Dazlich, D. A., Collatz, G. J., and Randall, D. A.: A revised land surface parameterization (SiB2) for atmospheric GCMs, 2. The generation of global fields of terrestrial biophysical parameters from satellite data, J. Climate, 9, 706–737, 1996a.

HESSD
9, 1163–1205, 2012

Sellers, P. J., Randall, D. A., Collatz, G. J., Berry, J. A., Field, C. B., Dazlich, D. A., Zhang, C., Collelo, G. D., and Bounoua, L.: A revised land surface parameterization (SiB2) for atmospheric GCMs, 1. Model formulation, J. Climate, 9, 676–705, 1996b.

Sen, O. L., Shuttleworth, W. J., and Yang, Z. L.: Comparative evaluation of BATS2, BATS, and SiB2 with Amazon data, J. Hydrometeorol., 1, 135–153, 2000.

Shangguan, W., Dai, Y., Liu, B., Ye, A., and Yuan, H.: A soil particle-size distribution dataset for regional land and climate modelling in China, Geoderma, doi:10.1016/j.geoderma.2011.01.013, in pess, 2011.

Soylu, M. E., Istanbulluoglu, E., Lenters, J. D., and Wang, T.: Quantifying the impact of groundwater depth on evapotranspiration in a semi-arid grassland region, Hydrol. Earth Syst. Sci., 15, 787–806, doi:10.5194/hess-15-787-2011, 2011.

Su, J.: Groundwater flow modeling and sustainable utilization of water resources in Zhangye Basin of Heihe River Basin, Northwestern China PHD, Cold and Arid Regions Environmental and Engineering Research Institute, Chinese Academy of Sciences, Lanzhou, China, 2005.

Su, Z.: The Surface Energy Balance System (SEBS) for estimation of turbulent heat fluxes, Hydrol. Earth Syst. Sci., 6, 85–100, doi:10.5194/hess-6-85-2002, 2002.

Twarakavi, N. K. C., Simunek, J., and Seo, S.: Evaluating interactions between groundwater and vadose zone using the HYDRUS-based flow package for MODFLOW, Vadose Zone J., 7, 757–768, doi:10.2136/vzj2007.0082, 2008.

van Genuchten, M. Th.: A closed-form equation for predicting the hydraulic conductivity of unsaturated soils, Soil. Sci. Soc. Am. J., 44, 892–898, 1980.

Vidale, P. L. and Stockli, R.: Prognostic canopy air space solutions for land surface exchanges, Theor. Appl. Climatol., 80, 245–257, 2005.

Wang, L., Koike, T., Yang, K., Jackson, T. J., Bindlish, R., and Yang, D. W.: Development of a distributed biosphere hydrological model and its evaluation with the Southern Great Plains Experiments (SGP97 and SGP99), J. Geophys. Res.-Atmos., 114, D08107, doi:10.1029/2008jd010800, 2009.

Wang, X. S.: AquiferFlow: a finite difference variable saturation three-dimensional aquifer groundwater flow model, China University of Geosciences (Beijing), Beijing, China, 2007.

Wang, X.-S., Ma, M.-G., Li, X., Zhao, J., Dong, P., and Zhou, J.: Groundwater response to leakage of surface water through a thick vadose zone in the middle reaches area of Heihe River Basin, in China, Hydrol. Earth Syst. Sci., 14, 639–650, doi:10.5194/hess-14-639-2010, 2010.

HESSD
9, 1163–1205, 2012

Wen, X. H., Wu, Y. Q., Lee, L. J. E., Su, J. P., and Wu, J.: Groundwater flow modeling in the Zhangye Basin, Northwestern China, Environ. Geol., 53, 77–84, doi:10.1007/s00254-006-0620-7, 2007.

Yang, K., Koike, T., Ye, B. S., and Bastidas, L.: Inverse analysis of the role of soil vertical heterogeneity in controlling surface soil state and energy partition, J. Geophys. Res.-Atmos., 110, D08101, doi:10.1029/2004jd005500, 2005.

Yeh, P. J. F. and Eltahir, E. A. B.: Representation of water table dynamics in a land surface scheme, Part I: Model development, J. Climate, 18, 1861–1880, doi:10.1175/jcli3330.1, 2005.

York, J. P., Person, M., Gutowski, W. J., and Winter, T. C.: Putting aquifers into atmospheric simulation models: an example from the Mill Creek Watershed, Northeastern Kansas, Adv. Water Resour., 25, 221–238, 2002.

Zhou, J., Hu, B. X., Cheng, G., Wang, G., and Li, X.: Development of a three-dimensional watershed modelling system for water cycle in the middle part of the Heihe rivershed, in the west of China, Hydrol. Process., 25, 1964–1978, doi:10.1002/hyp.7952, 2011.

Zhou, X. Z., Zhao, J. D., Wang, Z. G., Zhang, A. L., and Ding, H. W.: Investigation on assessment and utilization of groundwater resources in the middle reaches area of Heihe River Basin, in Gansu Province, The Second Hydrogeoloical and Engineering Geology Team, Gansu Bureau of Geology and Mineral Exploitation and Development, Zhangye, China, 1990.

HESSD

9, 1163–1205, 2012

Table 1. Details of the validation stations.

Station name	Longitude/ latitude	Ground-water table (m)	Ground-water depth (m)	Vegetation classification of SiB2	Model validation period
LZG	100.07/ 39.25	1388.7	1.8	Short vegetation/ C4 grassland	31 May to 14 Jul 2008 (soil moisture) 19 May to 27 Aug 2008 (ET)
ZYNOC	100.28/ 39.08	1433.8	26.4	Broadleaf shrub and bare soil	1 Jul to 30 Sep 2008
YK	100.41/ 38.86	1468.2	71.7	Agriculture/ C3 grassland	1 Apr to 1 Oct 2008

HESSD
9, 1163–1205, 2012

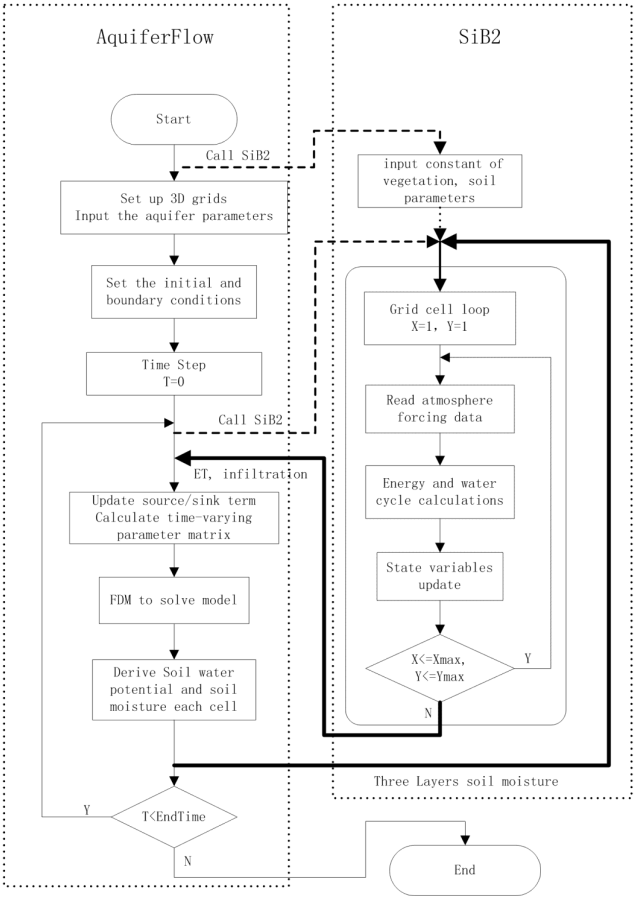

Fig. 1. Coupling between SiB2 and AquiferFlow in GWSiB. The black solid lines with arrows indicate the direction of the variable transmission, and the short dashed lines with arrows indicate the call of the function.

HESSD
9, 1163–1205, 2012

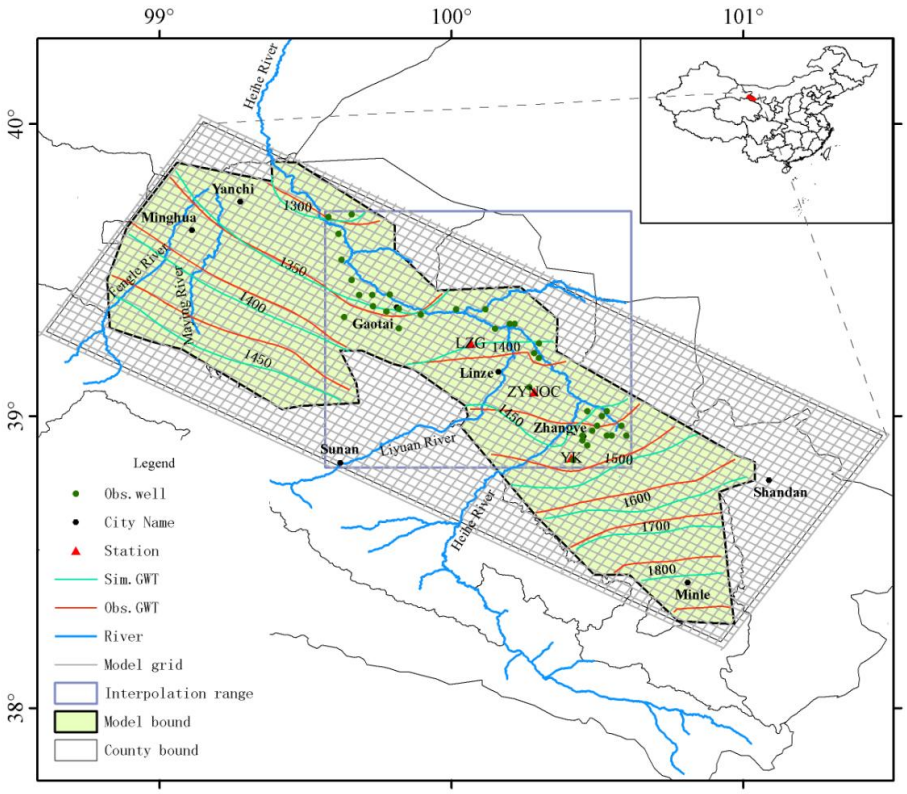

Fig. 2. The location of the study area and the simulated and the observed groundwater table (GWT) of study area in December 2008. The observed groundwater table within the scope of 36 wells (interpolation range) are obtained by the interpolation method; the rest of the study area's GWT are obtained by extrapolation.

HESSD
9, 1163–1205, 2012

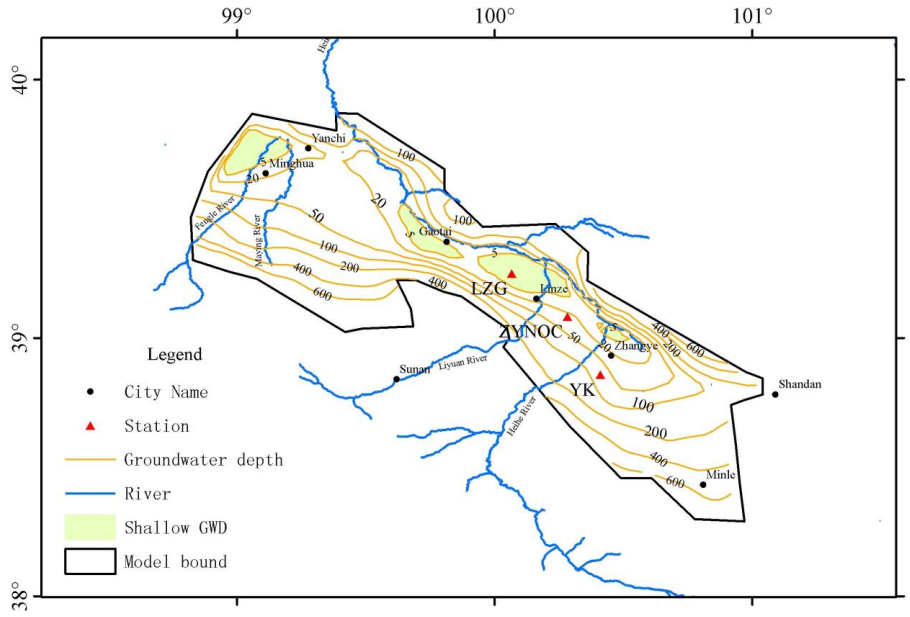

Fig. 3. Map of groundwater depth (GWD) and the location of validation stations.

HESSD
9, 1163–1205, 2012

Coupling a groundwater model with a land surface model

W. Tian et al.

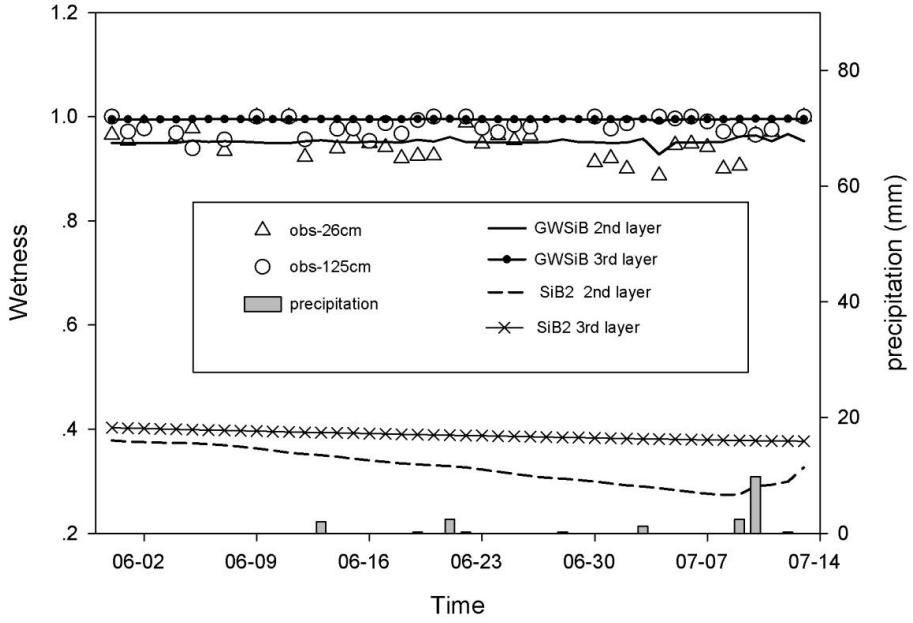

Fig. 4. Observed soil wetness at depths of 26 cm and 125 cm below the ground surface and the soil wetness of the second and third layers simulated with GWSiB and SiB2, and the precipitation in the Linze grassland station from 31 May 2008 to 13 July 2008.

HESSD
9, 1163–1205, 2012

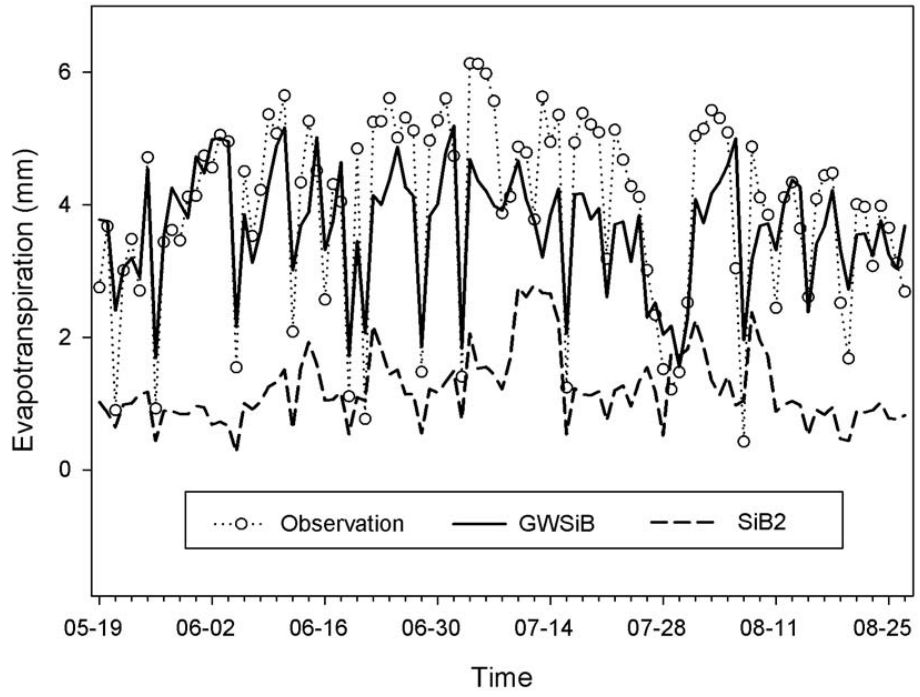

Fig. 5. Observed evapotranspiration, GWSiB-simulated evapotranspiration, and SiB2-simulated evapotranspiration in the Linze grassland station from 19 May 2008 to 27 August 2008.

HESSD
9, 1163–1205, 2012

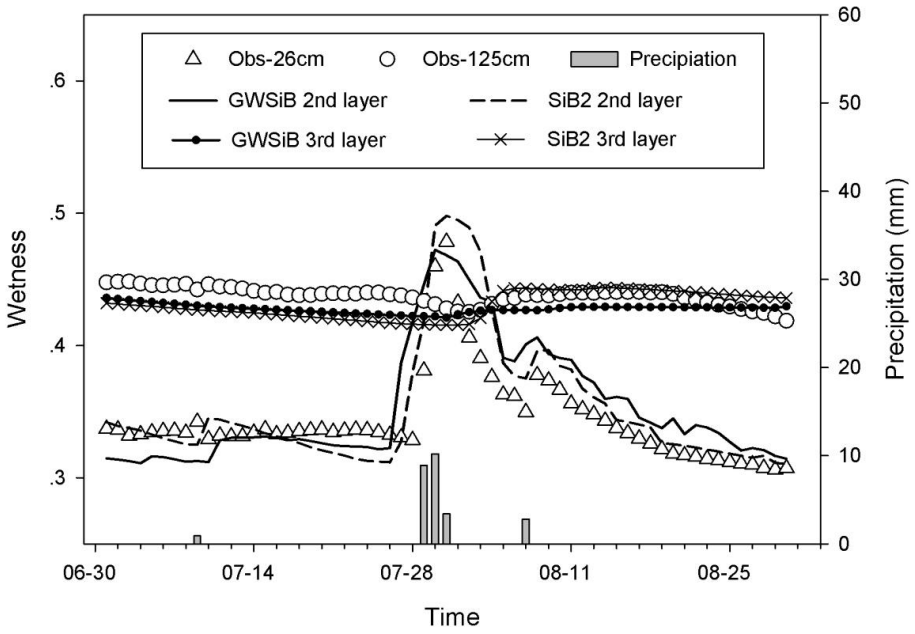

Fig. 6. Observed soil wetness at depths of 26 cm and 125 cm, the soil wetness in the second and third layers simulated with GWSiB and SiB2, and the precipitation data from the National Observatory on Climatology station at Zhangye from 1 July 2008 to 30 August 2008.

HESSD
9, 1163–1205, 2012

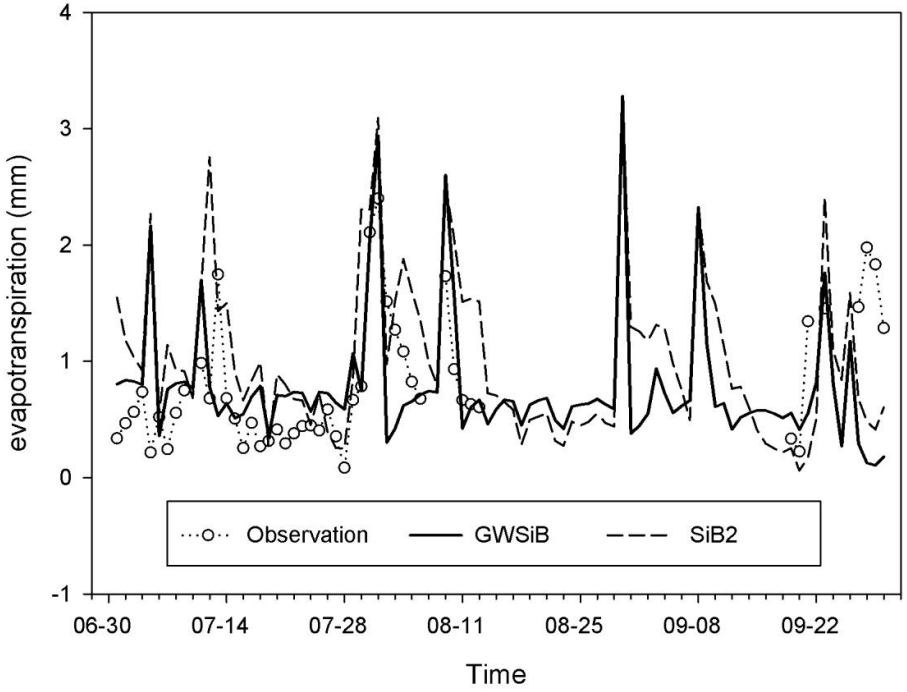

Fig. 7. Plot of the observed evapotranspiration, the GWSiB-simulated evapotranspiration, and the SiB2-simulated evapotranspiration from the National Observatory on Climatology station at Zhangye from 19 May 2008 to 27 August 2008.

HESSD
9, 1163–1205, 2012

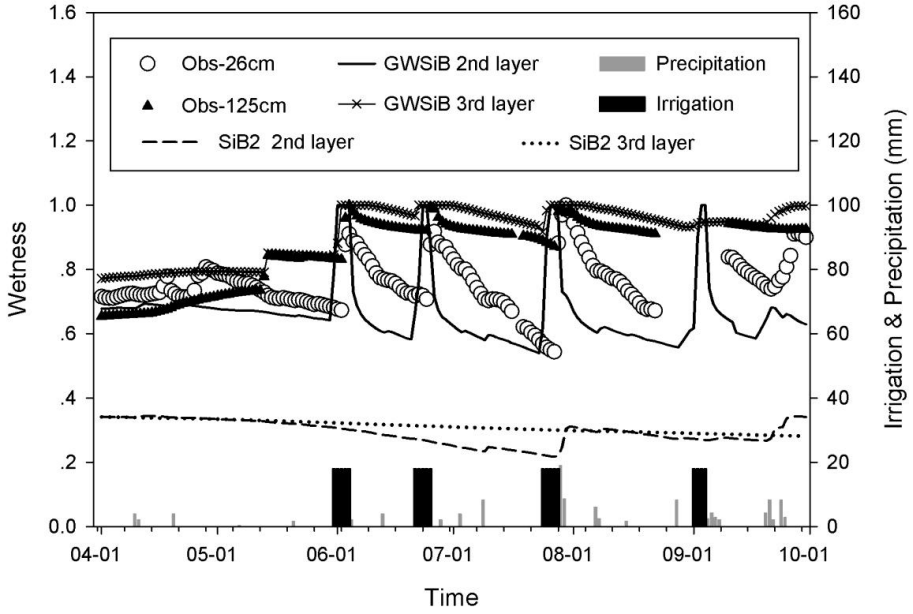

Fig. 8. Observed soil wetness at depths of 26 cm and 125 cm, the soil wetness in the second and third layers simulated with GWSiB and SiB2, the precipitation and the irrigation rate at the Yingke Station, Zhangye Oasis from 1 April 2008 to 1 October 2008.

HESSD
9, 1163–1205, 2012

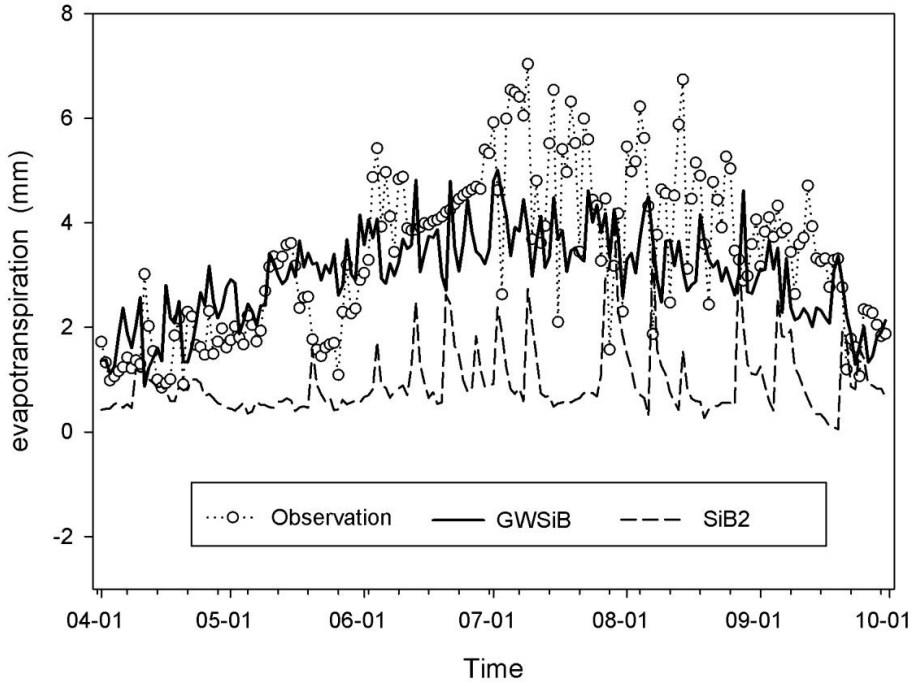

Fig. 9. Observed evapotranspiration, GWSiB-simulated evapotranspiration, and SiB2-simulated evapotranspiration at the Yingke Station, Zhangye Oasis from 1 April 2008 to 1 October 2008.

HESSD
9, 1163–1205, 2012

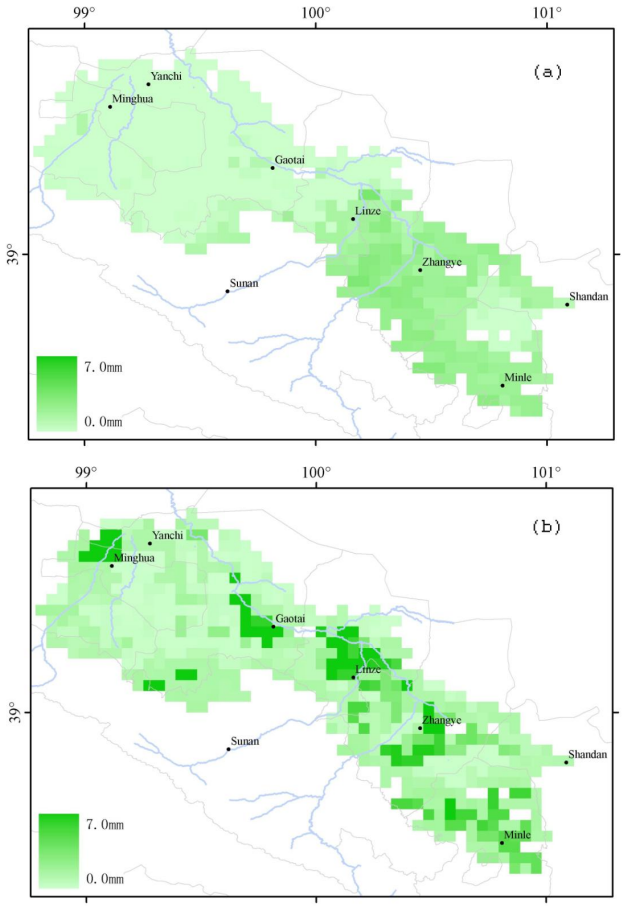

Fig. 10. Evapotranspiration simulated by **(a)** SiB2 and **(b)** GWSiB in the middle reaches of the Heihe River Basin on 24 June 2008.

HESSD
9, 1163–1205, 2012